An overview of :
A model independent calibration of quasars

Monthly
Notices
Of the
Royal
Astronomical
Society

Xiaolei Li, Ryan E. Keeley, Arman Shafieloo, Xiaogang Zheng, Shou Cao, Marek Biesiada, Zong-Hong Zhu5

Resources:
github.com/parsa-ghafour/Conferences_and_Seminars

At a glance:

Foreword	Base relation	Data sets	Calibration	Results
Important characteristics of quasars	Relation between the log of their ultraviolet (UV) and X-ray luminosities	Quasar sample (Training data set)	Unanchored luminosity distance	Model independent calibration results for the quasar parameters
Quasars as standardized candles	Free parameters	Supernovae Ia sample (Test data set)	Generating a set of cosmological functions	$\log{(D_L H_0)}$ - redshift relation
	Hyper parameters		GP regression	Residuals of the observed $\log{(F_X)}$ values with respect to the predicted $\log{(F_X)}$
Base relation			Reconstruct the expansion history	
Correlation between the Base relation and the cosmological distances			Likelihood	The linear relation between $\log{(L_{UV})}$ and $\log(L_X)$
			LINMIX_ERR	
			MCMC analysis	

Foreword:

Quasars

- Are luminous persistent sources
- Can be observed up to redshifts of $z \approx 7.5$ (Mortlock et al. 2011)
- Might be able to fill the redshift gap between the farthest observed Type Ia Supernovae and CMB (Scolnic et al. 2017)

Farthest SN Ia: $z \approx 2.3$ (ESA/Hubble, David O. Jones et al.)

CMB: higher redshift

Quasars can be used as standardized candles

Calibrate the largest quasar sample → Constraining the parameters of the Base relation → There is a strong correlation between the parameters characterizing the quasar luminosity relation and the cosmological distances

Base relation:

Quasars have also been used as standard candles whose standardization relies on the linear relation between the log of their ultraviolet (UV) and X-ray luminosities:

(Risaliti & Lusso 2015, 2017; Lusso & Risaliti 2016, 2017; Risaliti & Lusso 2019; Salvestrini et al. 2019; Lusso et al. 2019, 2020; Lusso 2020; Khadka & Ratra 2020a, b; Liu et al. 2020a, b, c; Geng et al. 2020; Zheng et al. 2021).

Slope

Offset

$$\log(L_X) = \gamma \log(L_{UV}) + \beta_1$$

rest-frame luminosities

Three free parameters

Hyperparameters

γ

β_1

Subparameter

δ

Is not shown directly in the equation

The intrinsic dispersion

Hyperparameters:

β_1 → Offset

Shifts the relation between the UV and X-ray luminosities up and down

β_1 is degenerate with H_0

Scales the corresponding distance-redshift relation up and down

γ → Slope

Split the quasar sample into subsamples(n)

Narrow redshift bins

For each subsample

Fit the base relation(n)

$$\underbrace{\gamma_1, \gamma_2, \gamma_3, ..., \gamma_n}$$

Average

(Risaliti & Lusso, 2019)

Data sets: (Training data set)

Quasar sample

Largest sample with both X-ray and UV

Total 12000 objects

Several filtering steps

Reduce the systematic effects

Final sample: 2421 quasars

$0.009 < z < 7.5$

30 quasars	XMM–Newton	(Nardini et al. 2019)
64 high-z quasars	Salvestrini et al	(Salvestrini et al. 2019)
840 quasars	XMM-XLL sample	(Menzel et al. 2016)
9252 quasars	SDSS-4XMM sample	(Mingo et al. 2016; Paris et al. 2017; Webb et al. 2020)
2392 quasars	Paris et al	(Paris et al. 2017, Evans et al. 2010)
15 local AGN	Lusso et al	(Lusso et al. 2020)

Data sets: (Test data set)

Supernovae Ia sample

↓

Pantheon SN Ia data set

↓

z_{max} = 2.26

(Scolnic et al. 2017; Liao et al. 2019, 2020; Rasmussen & Williams 2006, Holsclaw et al. 2010a, b, 2011, Shafieloo, Kim & Linder 2012, Joudaki et al. 2018, Keeley et al. 2019, 2020, 2021

Calibration:

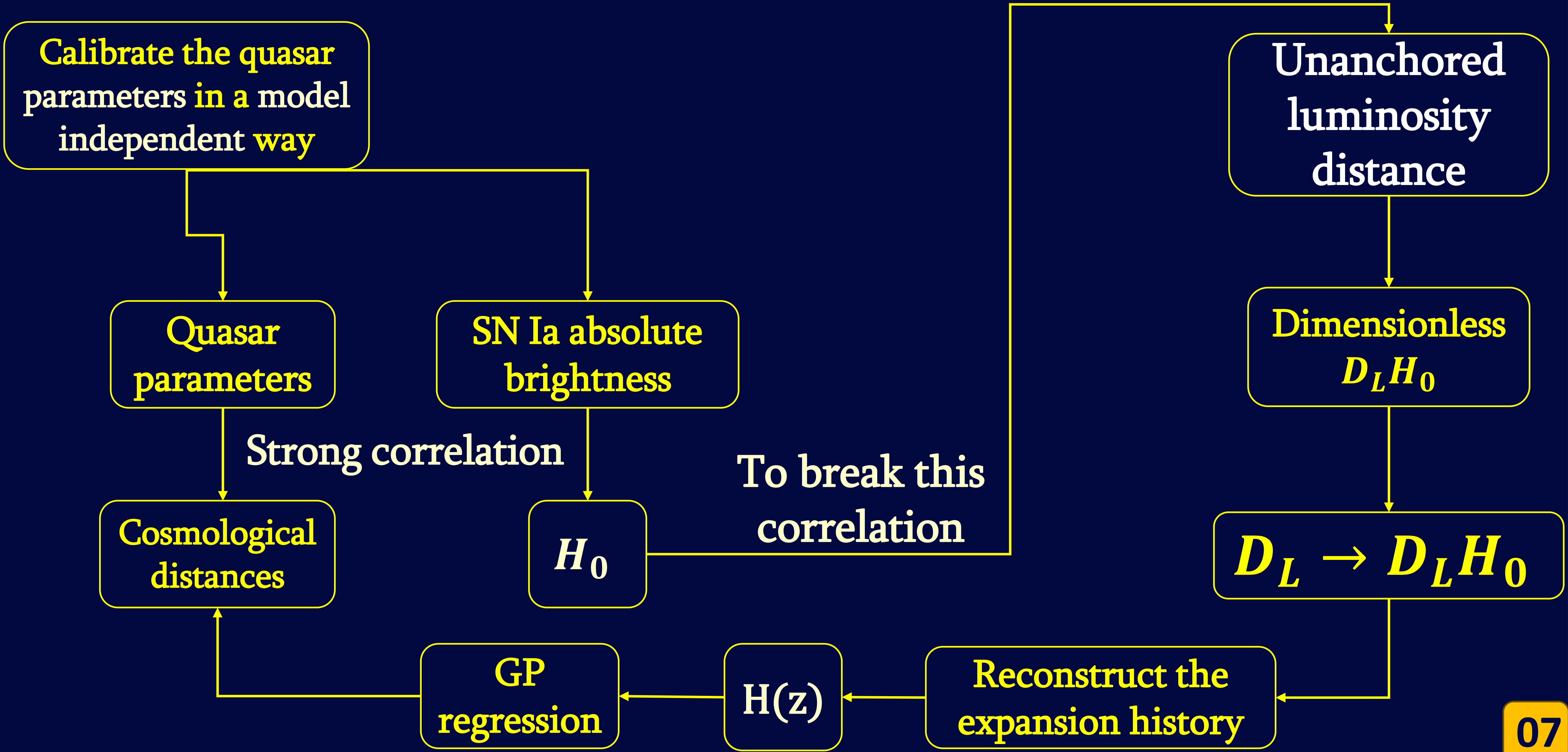

GP regression: (Gaussian Process regression)

Generating a set of cosmological functions

covariance function between the values at different redshifts

(Rasmussen & Williams 2006; Holsclaw et al. 2010a, b; Holsclaw et al. 2011; Shafieloo et al. 2012)

$$\langle\varphi(s_i)\varphi(s_j)\rangle = \sigma_f^2 \exp\left(-\frac{|s_i - s_j|^2}{2l^2}\right)$$

Hyperparameters

σ_f Amplitude of the fluctuations

l Coherence length of the fluctuations

$$s_i = \frac{ln(1+z_i)}{ln(1+z_{max})}$$

$$s_j = \frac{ln(1+z_j)}{ln(1+z_{max})}$$

$z_{max} = 2.26$

$$\varphi(s_i) \to \varphi(z)$$

$$\varphi(z) = ln\left(\frac{H^{mf}(z)}{H(z)}\right)$$

GP regression: (Gaussian Process regression)

Pantheon data set

SN Ia

Best fitting of ΛCDM model

True model should be very close to the flat ΛCDM model

Best fitting of the flat ΛCDM model from Pantheon

Mean expansion history function

$H^{mf}(z)$

Final reconstruction results are not quite independent

(Shafieloo et al. 2012; Shafieloo, Kim & Linder 2013; Aghamousa, Hamann & Shafieloo 2017)

GP regression: (Gaussian Process regression)

Unanchored luminosity distance

Dimensionless $D_L H_0$

$D_L \rightarrow D_L H_0$

$$\varphi(z) = ln\left(\frac{H^{mf}(z)}{H(z)}\right)$$

$$\varphi(z) \leftrightarrow H(z)$$

Integrate this function to get the unanchored luminosity distance

$$D_L H_0(z) = (1+z)\int_0^z \frac{c}{h(z)} dz$$

$$h(z) = \frac{H(z)}{H_0}$$

This function is directly constrained by the SN Ia data set and can be reconstructed

GP regression: (Gaussian Process regression)

GP calculates a posterior for $D_L H_0$ function

Posterior probability (Resources)

Revised or Updated probability

Updating the prior probability using Bayes' theorem (Resources)

$$P(A|B) = \frac{P(B|A)P(A)}{P(B)}$$

$$D_L H_0(z) = (1+z)\int_0^z \frac{c}{h(z)}dz$$

Posterior

$$P(D_L H_0|D_L) = \int \frac{\mathcal{L}\big(D_L H_0(\varphi)\big)P(\varphi)}{P(D_L)}$$

$\mathcal{L}\big(D_L H_0(\varphi)\big)$

Likelihood of the data

$P(\varphi)$

Consequence using a flat prior on the GP hyperparameters

Calibration:

Draw 1000 unanchored luminosity distances reconstructed from the SN Ia data

$$P(D_L H_0 | D_L) = \int \frac{\mathcal{L}\big(D_L H_0(\varphi)\big) P(\varphi)}{P(D_L)}$$

$D_L H_0$

Calculate the predicted quasar X-ray flux corresponding to these unanchored luminosity

$$\log(L_X) = \gamma \log(L_{UV}) + \beta_1$$

$$\begin{cases} log(F_X) = \gamma\, log(F_{UV}) + (2\gamma - 2) log(D_L) + \beta_2 \\ \beta_2 = \gamma log(4\pi) - log(4\pi) + \beta_1 \end{cases}$$

$$\begin{cases} log(F_X)^{SN} = \gamma\, log(F_{UV}) + (2\gamma - 2) log(D_L H_0) + \beta \\ \beta = \beta_2 - (2\gamma - 2) log(H_0) \end{cases}$$

Calibration:

$$log(F_X)^{SN} = \gamma\, log(F_{UV}) + (2\gamma - 2)log(D_L H_0) + \beta$$

$$log(F_X)^{QSO} = \gamma\, log(F_{UV}) + (2\gamma - 2)log(D_L H_0) + \beta$$

Compare

Likelihood

(Risaliti & Lusso 2015, and Lusso et al. 2020)

$$\mathcal{L}(\chi) = exp\left(-\frac{\chi^2}{2}\right)$$

$$\chi^2 = \sum_i \left[\frac{\left(\log(F_X(\gamma,\beta))_i^{SN} - \log(F_X(\gamma',\beta'))_i^{QSO}\right)}{s_i^2} + ln(s_i^2)\right]$$

$$s_i^2 = \sigma^2_{log(F_X)} + \gamma^2 \sigma^2_{log(F_{UV})} + \delta^2$$

Calibration:

$$s_i^2 = \sigma^2_{log(F_X)} + \gamma^2\sigma^2_{log(F_{UV})} + \delta^2$$

δ: Intrinsic dispersion

Reduce the Eddington bias

(Resources)

Measurement errors

Population characteristics

The observed dispersion of the X-ray fluxes is far larger than just the measurement error

LINMIX_ERR

(Kelly 2007) (Resources)

Effect of flattening

Must be some additional variance

An intrinsic feature of the quasar population

Calibration:

LINMIX_ERR

δ is only as large as it needs to be

$\delta \uparrow \; \sim \; s_i^2 \uparrow$

$$s_i^2 = \sigma_{log(F_X)}^2 + \gamma^2 \sigma_{log(F_{UV})}^2 + \delta^2$$

$s_i^2 \uparrow \sim \chi^2 \downarrow$

$$\chi^2 = \sum_i \left[\frac{\left(\log\left(F_X(\gamma, \beta)\right)_i^{SN} - \log(F_X)_i^{QSO} \right)}{s_i^2} + ln\left(s_i^2\right) \right]$$

$\chi^2 \downarrow \sim \mathcal{L}(\chi) \uparrow$

$$\mathcal{L}(\chi) = exp\left(-\frac{\chi^2}{2} \right)$$

Calibration:

Calculate the posterior distribution

- Slope
- Offset
- The intrinsic dispersion

- There is no evolution of the $L_{UV} - L_X$ relation with redshift
- The Hubble constant H_0 is absorbed into the parameter β

emcee
Python package
(Resources)

MCMC analysis
(Resources)

$1\sigma, 2\sigma, 3\sigma$ uncertainties

<u>Calibration:</u>

i. Draw 1000 unanchored luminosity distances from supernovae data

ii. Calculate the predicted quasar X-ray flux corresponding to these unanchored luminosity distances

iii. Define the likelihood of the quasar parameters

iv. Calculate the posterior distribution of the quasar parameters

$D_L H_0$ → ${F_X}^{QSO}$ → $\mathcal{L}(\chi)$ → MCMC

$$\gamma, \beta_1, \delta, 1\sigma, 2\sigma, 3\sigma$$

Results:

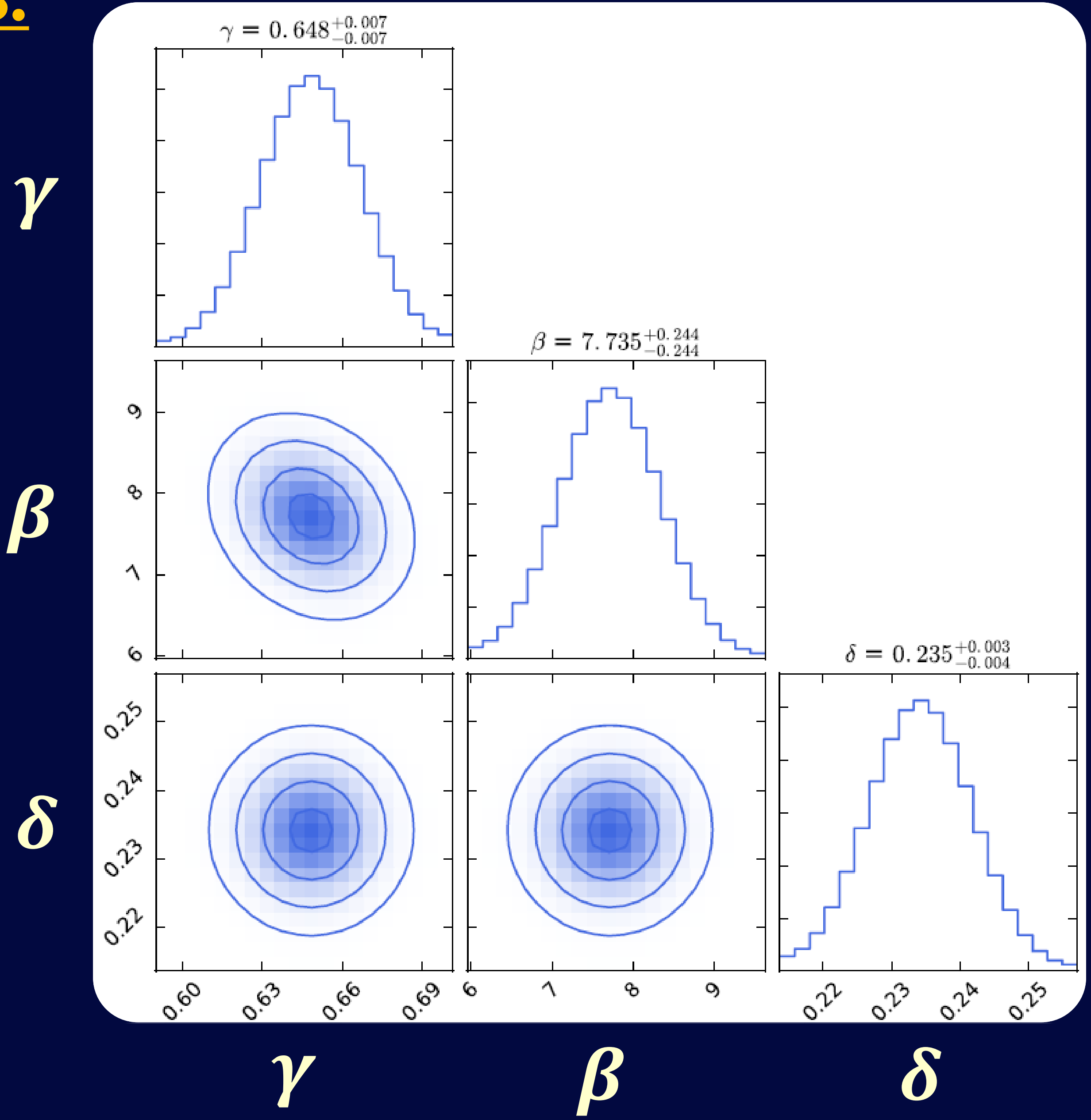

Model independent calibration results for the quasar parameters. GP regression reconstructions of $D_L H_0$ based on the Pantheon SN Ia compilation were used.
The contours represent the 1σ, 2σ, and 3σ uncertainties for γ, β, and δ.

Results:

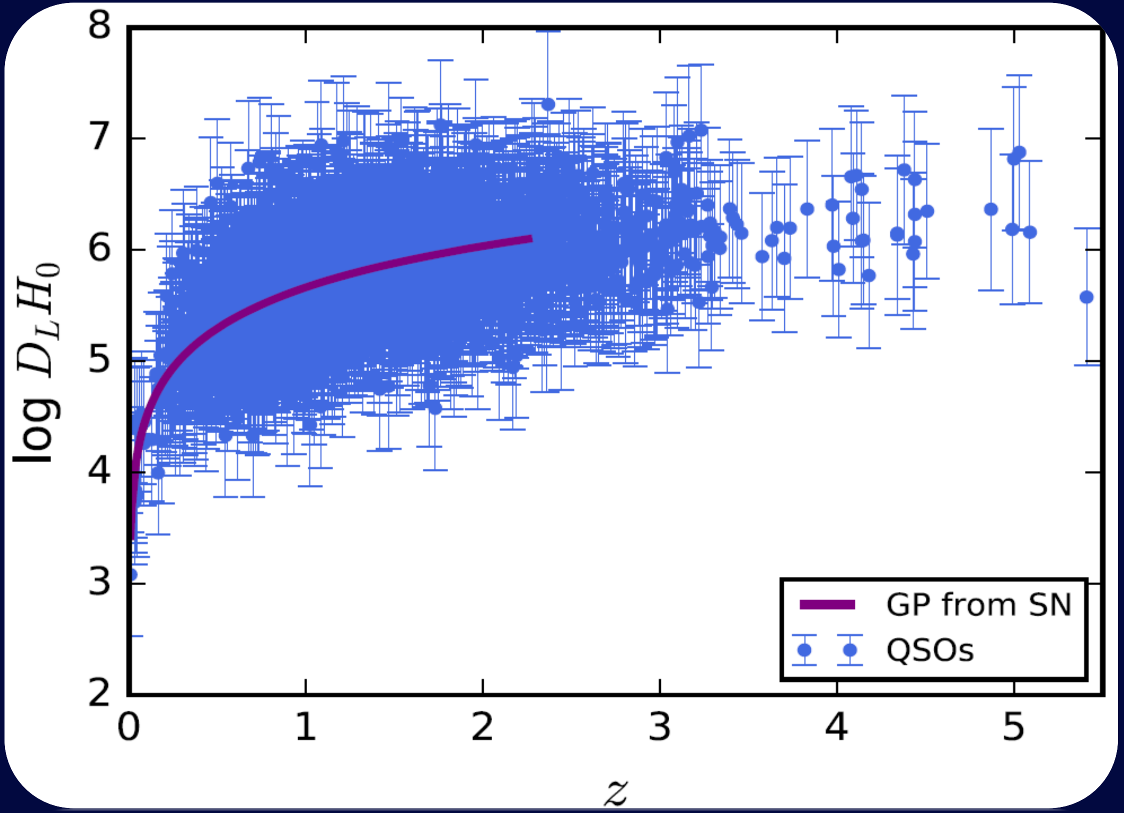

log $(D_L H_0)$-redshift relation for the 2421 calibrated quasars. The error bars of log $(D_L H_0)$ are obtained through error propagation and the purple solid line shows log $(D_L H_0)$ drawn from the posterior of the Pantheon compilation calculated with GP.

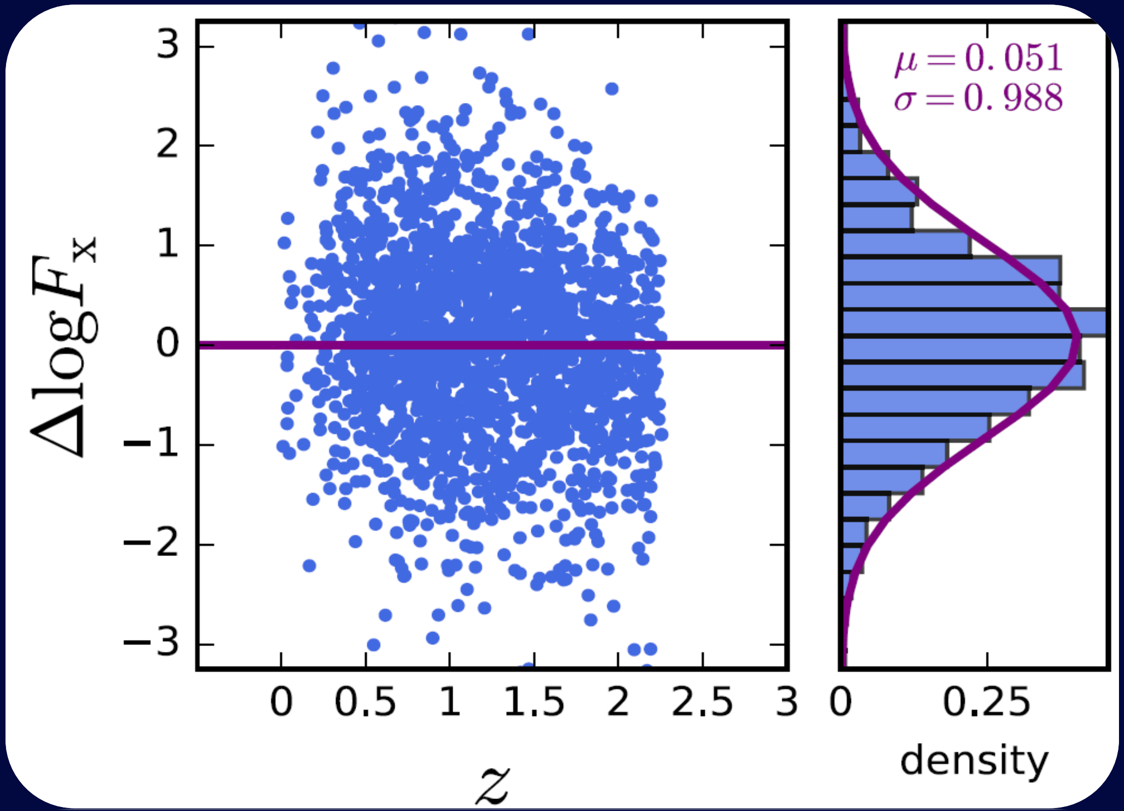

Residuals of the observed log (F_X) values with respect to the predicted log (F_X) values derived from the GP reconstructions of the Pantheon SN Ia compilation, normalized to the calibrated errors. The right plot shows the histogram for log (F_X) and the purple line shows the best Gaussian fit with $\mu = -0.051$ and $\sigma = 0.988$.

Results:

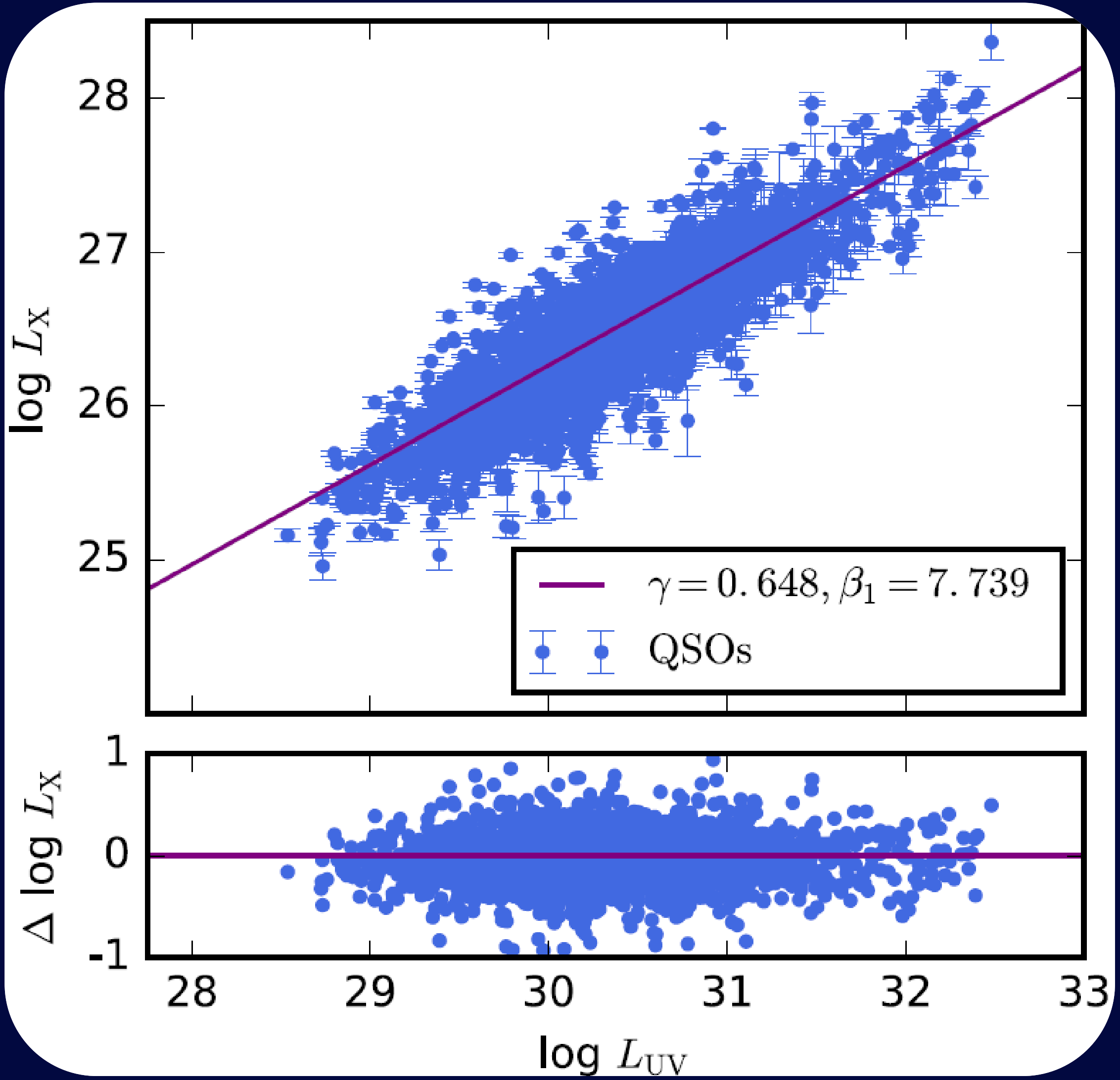

The linear relation between log (L_{UV}) and log(L_X) for the 2421 quasar sample we used. The purple solid line presents the best fit from our calibration results with slope γ = 0.648. The lower panel shows the residual of log (L_X) with respect to the best fitting results.